Received: 3 November 2023 | Revised: 12 January 2024 | Accepted: 12 January 2024

DOI: 10.1111/joa.14017

Journal of Anatomy ANATOMICAL SOCIETY WILEY

ORIGINAL ARTICLE

The changing morphology of the ventricular walls of mouse and human with increasing gestation

Bjarke Jensen[1] | Yun Hee Chang[1] | Simon D. Bamforth[2] | Timothy Mohun[3] | David Sedmera[4] | Martin Bartos[4,5] | Robert H. Anderson[2]

[1]Department of Medical Biology, Amsterdam Cardiovascular Sciences, University of Amsterdam, Amsterdam UMC, Amsterdam, the Netherlands

[2]Biosciences Institute, Faculty of Medical Sciences, Newcastle University, Newcastle, UK

[3]Crick Institute, London, UK

[4]Institute of Anatomy, First Faculty of Medicine, Charles University, Prague, Czech Republic

[5]Institute of Dental Medicine, First Faculty of Medicine, Charles University, Prague, Czech Republic

Correspondence
Bjarke Jensen, Amsterdam UMC, Department of Medical Biology, Meibergdreef 15, 1105AZ Amsterdam, the Netherlands.
Email: b.jensen@amsterdamumc.nl

Abstract

That the highly trabeculated ventricular walls of the developing embryos transform to the arrangement during the fetal stages, when the mural architecture is dominated by the thickness of the compact myocardium, has been explained by the coalescence of trabeculations, often erroneously described as 'compaction'. Recent data, however, support differential rates of growth of the trabecular and compact layers as the major driver of change. Here, these processes were assessed quantitatively and visualized in standardized views. We used a larger dataset than has previously been available of mouse hearts, covering the period from embryonic day 10.5 to postnatal day 3, supported by images from human hearts. The volume of the trabecular layer increased throughout development, in contrast to what would be expected had there been 'compaction'. During the transition from embryonic to fetal life, the rapid growth of the compact layer diminished the proportion of trabeculations. Similarly, great expansion of the central cavity reduced the proportion of the total cavity made up of intertrabecular recesses. Illustrations of the hearts with the median value of left ventricular trabeculation confirm a pronounced growth of the compact wall, with prominence of the central cavity. This corresponds, in morphological terms, to a reduction in the extent of the trabecular layer. Similar observations were made in the human hearts. We conclude that it is a period of comparatively slow growth of the trabecular layer, rather than so-called compaction, that is the major determinant of the changing morphology of the ventricular walls of both mouse and human hearts.

KEYWORDS
cardiac morphogenesis, compaction, excessive trabeculation, heart development, ventricular trabeculation

1 | INTRODUCTION

Differential growth rates have long been viewed as a major transformative factor of morphological change, both in ontogeny and evolution (Gould, 1966). In humans, the tremendous growth involved in transforming the fertilized egg into a neonate weighing approximately 3.5 kilograms allows for a great scope for such differential rates to impact on morphology, including the proportions of the

organs and their size (de Bakker et al., 2016). For the heart, much of the transformation from the stage of a tube with a solitary lumen to the 4-chambered organ can be attributed to the rapid growth of the chamber walls, which 'balloon' out from the slow-growing primary myocardium that constitutes the walls of the heart tube (Moorman & Christoffels, 2003). This growth is driven by cardiomyocytic proliferation, which itself is governed by evolutionarily-conserved transcriptional networks (de Boer et al., 2012; Jensen et al., 2013; Sedmera et al., 2003; Tian et al., 2017; Wang et al., 2018). Recently, using developmental series of human, mouse, shrew and chicken hearts, differential growth rates were shown to explain much of the gestational change found in the ratio of the width of the trabecular and compact components of the ventricular walls (Chang et al., 2022; Faber, Wüst, et al., 2022). The ratio of trabecular-to-compact myocardium is important in so far that it is a widely used metric for diagnosing so-called left ventricular non-compaction cardiomyopathy, notwithstanding that the diagnosis of this alleged entity has become controversial because of a very substantial rate of overdiagnosis (Anderson et al., 2017; Ross et al., 2020). In fact, the mere presence of excessive trabeculation can be considered to be without prognostic value (Aung et al., 2020; Petersen et al., 2023).

Non-compaction should be understood as the absence of compaction (Chin et al., 1990). Compaction itself is a process to which much importance has been assigned in transforming the highly trabeculated embryonic cardiac ventricular walls to the walls as seen in fetal and postnatal hearts, which are dominated by the thickness of the compact myocardium (Shi et al., 2023). What is entailed by alleged compaction varies between definitions (Wilsbacher & McNally, 2016). Most often, it is thought to involve the coalescence of trabeculations to produce the compact wall. The morphometric support for this process is weak (Faber, D'Silva, et al., 2021). The morphometric consequences of compaction, if they occurred, would be thickening of the compact layer by a reciprocal reduction of the trabecular layer, a reduction in the number of trabeculations and a reduction in the number and size of the intertrabecular recesses (Faber, D'Silva, et al., 2021). Because the apical components of the human ventricles exhibit the highest trabecular-to-compact ratio, it is thought that compaction is least extensive in these regions and most extensive at the ventricular base (Finsterer et al., 2017; Hussein et al., 2015; Sedmera et al., 1999).

Quantifications, such as those mentioned above, can in principle measure key aspects of compaction, as well as differences in the rate of growth of the trabecular and compact layers. For example, a decrease in the volume of trabecular myocardium could indicate compaction, whereas an increase in trabecular volumes would indicate growth. Compaction was initially quantified in chicken embryos. Specifically, the right ventricular free wall was assessed, which, in the adult bird, is very sparsely trabeculated, even when compared to the parietal wall of the neighbouring left ventricle (Rychterova, 1971). Compared to many mammalian species, chicken is an extreme case simply because of these differences in trabeculation (Rowlatt, 1990). Indeed, the setting in human is the inverse, since the right ventricle is more trabeculated than the left ventricle (Riekerk et al., 2022). Shrews, a group of tiny mammals, quite resemble chickens in the sparseness of trabeculation in the right ventricle, but the thickening of their compact wall during gestation occurs at a time when the trabecular layer itself is also increasing in width and volume (Chang et al., 2022). Compaction, then, can play a role in cardiogenesis (Hanemaaijer et al., 2019). The magnitude of the process, however, is much more ambiguous when considering the extent to which it applies to various mammalian species, particularly humans. Perhaps the most used measure of compaction is the trabecular-to-compact ratio. This measurement is itself a challenge. Should the value be interpreted as relating to the width of the trabecular layer as the numerator, the compact layer as the denominator or both? This challenge is particularly acute concerning developmental studies, since the ratio changes dramatically during the continuous growth of the trabecular and compact layers, both in humans (Blausen et al., 1990; Faber, Wüst, et al., 2022) and in mice (Ishiwata et al., 2003).

Many of the quantifications on mouse and human ventricular mural development concern measurements of width or area on histological sections. It is these measurements that changes in volume have been inferred from. A key motivation for the present study, therefore, was to provide volumetric data on ventricular mural development. Volumetric data can aid the interpretation of changes in morphology and morphogenetic processes such as apoptosis, remodelling and thickening could reflect a reduction, no change or increase in tissue volume respectively. While histological 4-chamber views are often shown, there is a dearth of standardized images in short-axis views and in long-axis views in particular. A second key motivation for the present study was to provide a comprehensive set of standardized images of the changing morphology, with increasing gestation, of the ventricular walls of mouse and human hearts. Here, we used a comparatively large dataset of high-resolution images of mouse hearts, supplemented with data from human hearts, to quantify the changes in the extent of the trabecular and compact layers. These changes coincide with the proportional reduction of the trabecular layer that is interpreted as compaction. For the mouse, we investigated embryonic, fetal and early postnatal hearts, as well as adult hearts. For the human hearts, we investigated embryonic stages, along with fetal hearts from the first trimester. We show that the changes interpreted as compaction are found during a period of relatively slow growth of the trabecular layer.

2 | MATERIALS AND METHODS

2.1 | Specimens

We have inspected visually over 450 datasets prepared by high-resolution episcopic microscopy showing the structure of the developing heart in wild-type mice of an outbred background (NIMR Parkes) from embryonic day (E) 10.5 to postnatal day 3. From these samples, we (RHA) chose, on morphological grounds such as the absence of blood clots and artefactual collapse of chamber walls, 5 appropriate datasets for each of the days of development. The sex of the

specimens was not determined. This yielded a total of 50 hearts, all of which were visualized in standardized views, thus permitting quantification of the amount of trabecular as opposed to compact myocardium. The mice had been collected as part of an extensive study of normal and abnormal cardiac development undertaken initially at the National Institute of Medical Research and continued subsequent to the transfer to the Crick Institute in London. Human embryos, covering the Carnegie stages (CS) from 11 through 17 and two early fetal stages, were obtained from the Human Developmental Biology Resource funded by the MRC/Wellcome-Trust, and maintained at Newcastle University (www.hdbr.org) (CS11 $n=1$; CS12 $n=1$; CS13 $n=3$; CS14 $n=3$; CS15 $n=3$; CS16 $n=2$; CS17 $n=1$; and one specimen from post-conception weeks 8 and 11). The sex of the specimens was not determined. All the samples were imaged using high-resolution episcopic microscopy and micro-computed tomography techniques as previously described (Anderson & Bamforth, 2022; Degenhardt et al., 2010; Geyer et al., 2009). The spatial resolution was such that any trabeculation was visualized on many voxels. The highest spatial resolution was used for E10.5 ($1.61\times1.61\times1.29\,\mu m$), at which age trabeculations are some 15–20 μm wide, and the lowest was used for postnatal day 3 ($6.57\times6.57\times3.00\,\mu m$). The median spatial resolution of the 50 image stacks was $3.39\times3.39\times2.00\,\mu m$. Stacks of intrinsically aligned serial images were subsampled and converted into volume data sets and analysed using Amira software (ThermoFisher Scientific). Three-dimensional images were created by manual segmentation using the label field function of Amira.

2.2 | Micro-computed tomography

The hearts of six adult mice (15 months) of either sex were perfused in Langendorff mode for the purposes of optical mapping of electrical impulse propagation (Olejnickova et al., 2021) followed by fixation for 24 h in 4% paraformaldehyde in PBS at 4 C. The hearts were then processed for micro-computed tomographic (CT) examination essentially as described recently (Gregorovicova et al., 2022), keeping the specimens in iodine solution for 1 month. The specimens were scanned in a plastic tube immersed in phosphate-buffered saline with the following scanning parameters: pixel size = 7.5 μm, source voltage = 90 kV, source current = 111 μA, filter: Al 0.5 mm + Cu 0.038 mm, rotation step = 0.2°, frame averaging = 2, specimen rotation of 180°, camera binning 2 × 2, scanning time = approx. 3 h per specimen. Flat-field correction was updated prior to each scanning. Scans were acquired using SkyScan 1272 (Bruker micro-CT, Belgium). Projection images were reconstructed with NRecon (Bruker micro-CT, Belgium) with the adequate setting of correction parameters (misalignment, smoothing, ring-artifact correction and beam hardening). 3D visualization was created by CT Vox (Bruker micro-CT, Belgium). CTAn (Bruker micro-CT, Belgium) was used to perform image processing.

2.3 | Quantifications

To quantify the volume of the trabecular and compact layers per ventricle per specimen, image stacks were imported to Amira (v2020.2, Thermo-Fisher). On equidistant images, either in the transverse or frontal plane of the heart, we labelled the trabeculations as opposed to the compact layers of the walls of both left and right ventricles. The hearts were generally clear of blood coagulates, permitting visualization of the full depth of most intertrabecular recesses. In this way, the intertrabecular recesses mark the trabecular layer as distinct from the compact layer, which is free of recesses (Figure 1). Approximately 10 equidistant images were labeled for each heart (Figure 1). The spaces between the images varied between the investigated stacks primarily because of differences in size of the heart, but also because of differences in spatial resolution. The labelled areas relate to the true volume, according to Cavalieri's principle (Gundersen et al., 1988) or Simpson's rule, with an error of approximately 10%. Volume readouts of the labels were derived from the

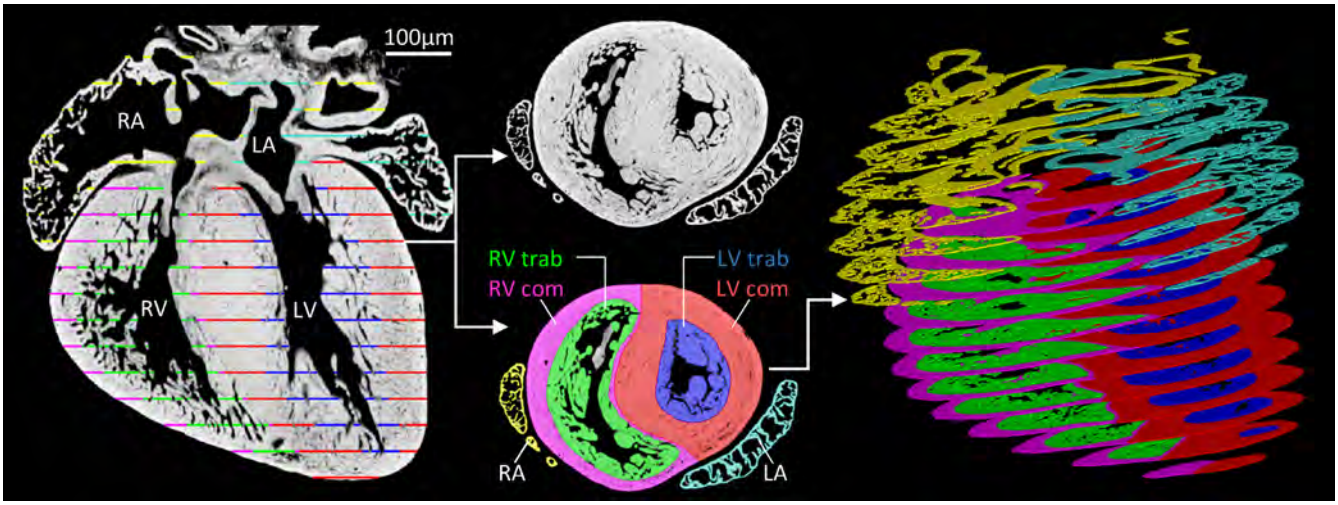

FIGURE 1 Workflow of myocardial volume quantifications. Approximately 10 equidistant images were chosen (left image) for labelling of trabecular (trab) and compact (com) myocardium of the left ventricle (LV) and right ventricle (RV). LA, left atrium; RA, right atrium.

Materials Statistics module in Amira. They were then multiplied by the space between the labelled images.

Especially the embryonic hearts were quite uniform in appearance, whereas the oldest hearts could have somewhat folded walls, but it has previously been shown that only gross mislabeling can substantially change the growth trajectories of fast-growing myocardium (Faber, Wüst, et al., 2022). This change in morphology suggested that the state of contraction of the fixed hearts may increase with development. To obtain a quantitative correlate of contraction, we measured the volume of the intertrabecular recesses and the central cavity. This was done in the image stacks, one per age, in which we measured the median value of the trabecular proportion of left ventricular myocardium. By correlating the volume of the intertrabecular recesses to developmental time, we could test whether intertrabecular recesses disappear. In this regard, a lower volume could be interpreted to demonstrate the disappearance of recesses. By dividing the total ventricular cavity volume by the total ventricular myocardial volume, we could test whether the ages exhibit differences in state of contraction. A lower volume could then be interpreted as indicating a greater state of contraction. Correlations were calculated with a linear regression analysis in Excel 2016 (Microsoft).

So as to provide images, episcopic datasets were acquired for each day of development from embryonic (E) day 10.5 to the end of gestation, which for the mouse is equivalent to E18.5. An additional dataset was examined from the third postnatal day. For each dataset, orthogonal sections were prepared in the frontal, sagittal and short axis planes, as far as possible obtaining comparable sections for each dataset. The short axis sections originated from approximately mid-height in the apical region, where the apical region, in the fetal and postnatal hearts, can be defined as the part of the ventricle that is apical to the papillary muscles. Image stacks were imported using Osirix (Pixmeo SARL, Switzerland) software to create three-dimensional datasets, from which the images in orthogonal planes were selected.

3 | RESULTS

3.1 | Quantifications of murine ventricular mural development

The volume of the trabecular and compact layers increases manyfold from the smallest and youngest hearts, from 10.5 days since conception, to the ones obtained on neonatal day 3 (Figure 2). Compared to the left ventricle, the right ventricle attains a greater volume of trabeculations and a smaller volume of compact muscle. Consequently, in the later stages, the right ventricle has a greater layer of trabecular myocardium compared to compact myocardium than does the left ventricle. In the early stages, the walls of both ventricles are composed primarily of trabecular myocardium, with three-quarters of the ventricular mass being occupied by trabeculations. By the third neonatal day, the trabeculations make up only about two-fifths of the volume of the right ventricular wall and one-fifth of the volume of the left ventricular wall (Figure 2). This decrease in proportional trabeculation, however, is not brought about by a decrease in the volume of the trabeculations, as would be expected if the decrease was the outcome of coalescence of pre-existing trabeculations, or so-called 'compaction'. Instead, the compact layer of the wall grows at a greater pace than does that of the trabeculations. Hence, it is the differential rate of growth that drives the reduction in proportional trabeculation (Figure 2).

Having assessed the arrangement of the walls, we next quantified the volume of the intertrabecular recesses and central cavity of both ventricles of the one heart per stage that had the median value of left ventricular trabeculations (Figure 3). When the volumes of the ventricular cavity were normalized to the volumes of ventricular myocardium, these ratios, for the early periods, were intermediate in value to those of end-diastolic and end-systolic left ventricles of adult humans (Figure 3b). In the fetal stages, the ratios decreased well below that of the end-systolic value, suggesting that the fetal ventricles were much more contracted than the embryonic hearts (Figure 3b). Despite a likely greater state of contraction in the older and bigger hearts, we found a greater volume of the central cavity and intertrabecular recesses (Figure 3c). Proportionally, however, the intertrabecular recesses were smaller in the older hearts.

Taken together, all myocardial and cavity volumes increase in development. Concomitantly, there is a decrease in the proportion that the trabeculations contribute to the ventricular walls. There is also a decrease in the proportion that the intertrabecular recesses contribute to the ventricular lumens. So as to provide a pictorial account of the changes, we chose, on the basis of the proportional changes, the median trabeculated specimen for each day of development so as to obtain the orthogonal planes through the left ventricle.

3.2 | Morphological description of murine ventricular wall development

Virtual sections were made for all five hearts for each of the periods from E10.5 through E18.5, and then comparable sections for the hearts obtained on the third postnatal day. Because of the pronounced changes in the anatomical arrangement of the ventricular walls during the periods from E13.5 to E15.5, it was difficult to provide comparable images for each specimen. Assessment of the datasets, however, showed that the specific plane of sectioning made little difference to the perceived thicknesses of the different layers. The hearts shown in Figures 4–6, therefore, are those with the median value of proportional left ventricular trabeculation for each day. As explained, for each dataset we prepared sections through the left ventricle in short-axis, four-chamber and long-axis planes.

At the beginning of development, from E10.5 through E13.5, the ventricular walls are composed primarily of trabeculations (Figure 4). This coincides with the noted increase in trabecular mass (Figure 2). During the same period, nonetheless, we also observed a substantial increase in the volume of compact muscle (Figure 2). This change

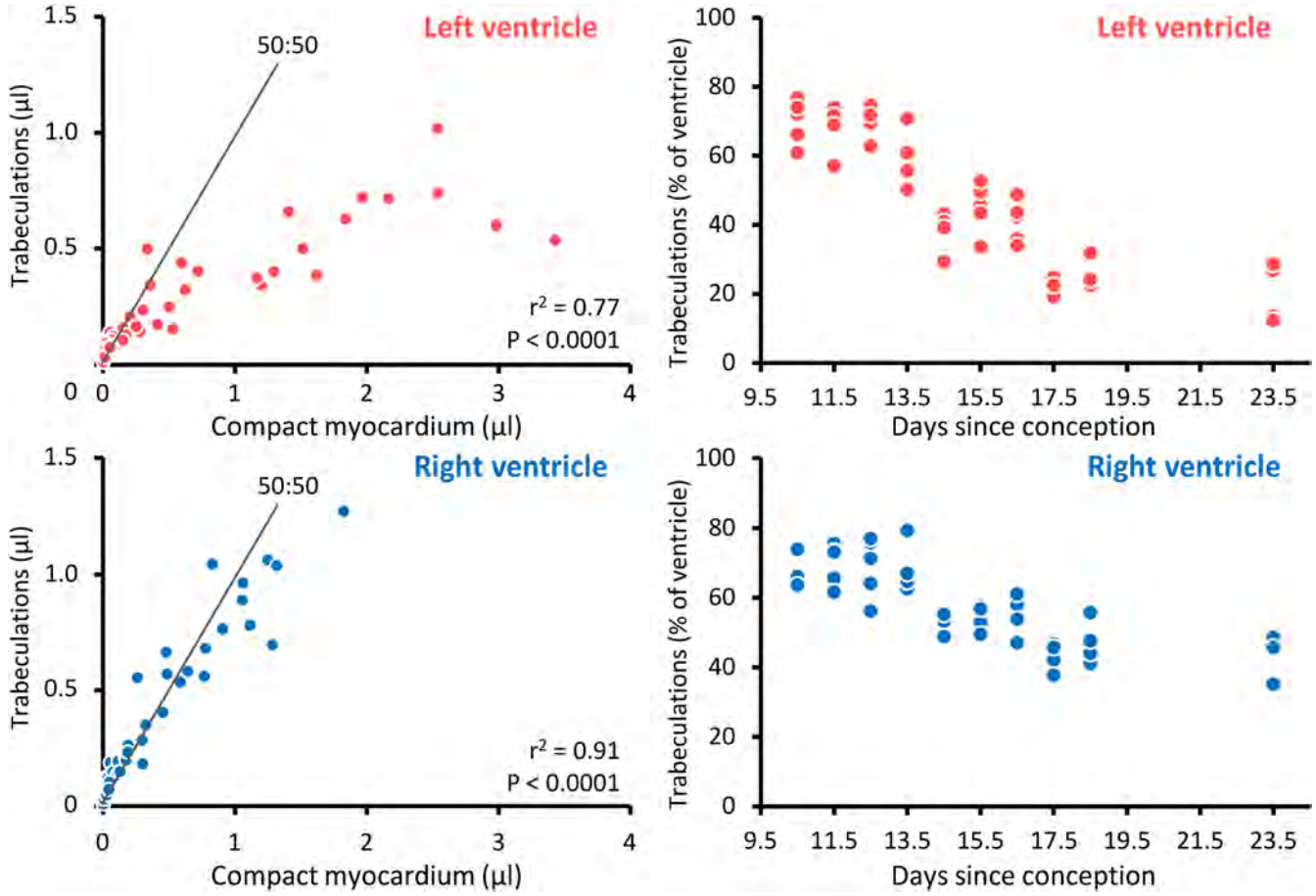

FIGURE 2 Change in trabecular volume and proportion in mouse heart development. Notice the strong positive and significant correlations between the volumes of compact and trabecular myocardium ($N = 50$; $N = 5$ per day). This demonstrates that compaction, if measurable as a drop in trabecular volume and reciprocal increase in compact volume, does not drive the growth of the compact wall. The line 50:50 indicates the relation at which trabecular and compact myocardium have the same proportion.

is most apparent when inspecting the ventricular septum (Figure 4, E13.5, label VS). It is during E13.5 that so-called 'compaction' is alleged to contribute to the thickening of the compact wall (Faber, D'Silva, et al., 2021). Our data do not support that claim. A process of coalescence of trabeculations (Henderson & Anderson, 2009) is seen to occur so as to produce the papillary muscles of the atrioventricular valves, with a similar process producing the future septomarginal and septoparietal trabeculations of the right ventricle. None of this myocardium, however, is incorporated into the compact layer of the ventricular walls, but rather remains as trabeculated myocardium. The sides of the crest of the ventricular septum are also surmounted by trabeculations in the earliest stages. By E13.5, the septal crest is draped with only a thin layer of trabeculations. A significant portion of the initial trabeculations do not disappear, but instead become the branches of the atrioventricular conduction axis (van Weerd & Christoffels, 2016). Because of their low rate of growth, these surface trabeculations eventually become tiny when compared to the large bulk of the septum.

By E14.5, the central cavities of both ventricles are much expanded (Figures 4, 5). This change has previously been measured as a decrease in the proportion that intertrabecular recesses compose of the total left ventricular cavity (Jensen et al., 2016). During this period, there is also a significant increase in the thickness of the compact layer itself. By E16.5 (Figure 5), the papillary muscles have become much thicker than the neighbouring trabeculations. This finding shows that trabeculations themselves can grow well beyond their previous diminutive size without becoming incorporated into the compact layer of the wall. During the same stages, there is also a further 'laying down' of the bundle branches on either side of the ventricular septum (Sankova et al., 2012). These changes are seen to continue during E17.5 (Figure 5). By this stage, when assessed in the short axis, the apical trabeculations are now no more than excrescences on the endothelial surface of the ventricular cavity, although when seen in the four-chamber view, they provide a lace-like configuration in the right ventricle. By this stage, despite a high number of trabeculations, the compact layer has now increased markedly in thickness and is also much greater in volume (Figure 2), with the proportion of trabecular muscle much lowered (Figure 2). During the period of transition from embryonic to fetal growth, therefore, major changes are seen towards the adoption of the adult morphology, albeit without overt evidence of coalescence of trabeculations into the compact layer of the wall.

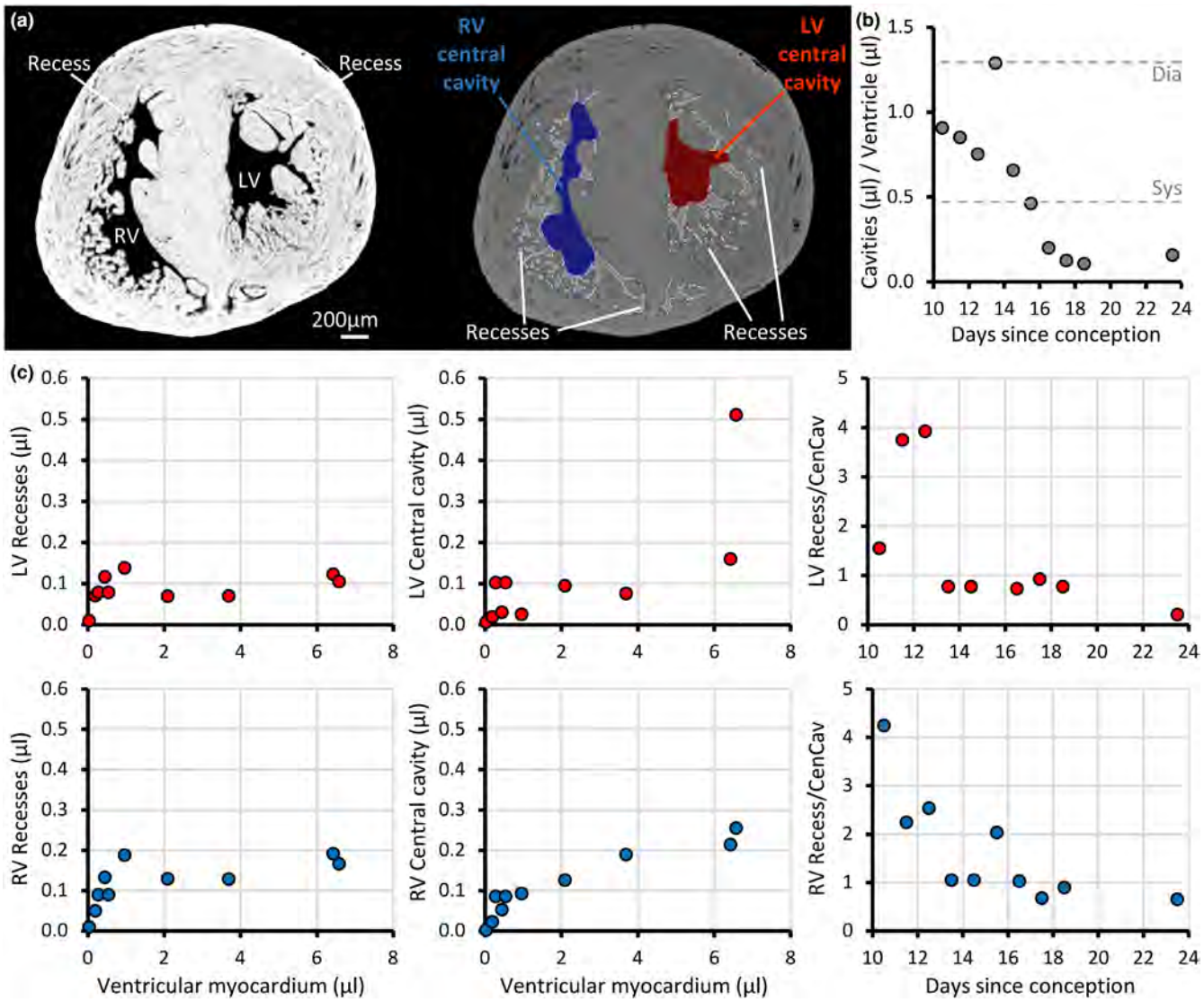

FIGURE 3 Gestational changes in the volumes of the ventricular cavities in mice. (a) Short-axis mid-ventricular section of the E18.5 mouse ventricle, showing the labelling of central cavity and intertrabecular recesses. (b) Lines Dia and Sys refer to the ratio derived from dividing the adult human normal value of both sexes of left ventricular end-diastolic volume (Dia) and end-systolic volume (Sys) by the left ventricular mass (adapted from values from [Luu et al., 2022]; The values are much the same in children [van der Ven et al., 2020]). In the mouse fetuses, the ratio of cavities to ventricular myocardial volume is well below the Sys line, suggesting these ventricles are much contracted. (c) Gestational increase of the volume of the intertrabecular recesses and central cavity of both the left (red) and right ventricle (blue). There is a pronounced decrease in the proportion that the intertrabecular recesses comprise out of the total ventricular cavity.

Towards the end of gestation, the compact layers of the ventricular walls begin to show aggregation of their contained cardiomyocytes into sheets (Figure 6). This remodelling is found exclusively within the compact wall, but does show some resemblance to a trabecular pattern. By the time of birth, the trabeculations are barely recognizable when compared to the thickness of the compact wall and the size of the ventricular cavity. The trabeculations, nonetheless, can still be recognized at the apex, with this feature seen in short-axis and long-axis cuts. They are particularly prominent beneath the bases of the papillary muscles, where they 'cushion' the base of the muscles from the supporting compact layer of the walls. This perceived reduction in the trabecular layer is in part an effect of inspecting thin sections. Visualizations of the whole wall reveal a high number of trabeculations, even in the ventricular base

FIGURE 4 Embryonic development of the ventricular walls of the mouse heart from Embryonic day (E) 10.5 through 13.5. Each row shows the orthogonal sections of the chosen dataset. The left-hand column shows the short axis plane at more or less the middle part of the ventricle. The middle columns show the so-called 'four chamber' views, which are essentially coronal cuts through the cavity of the left ventricle. The right-hand columns then show the cut across the long axis of the left ventricle. LV, left ventricle; RV, right ventricle; VS, ventricular septum.

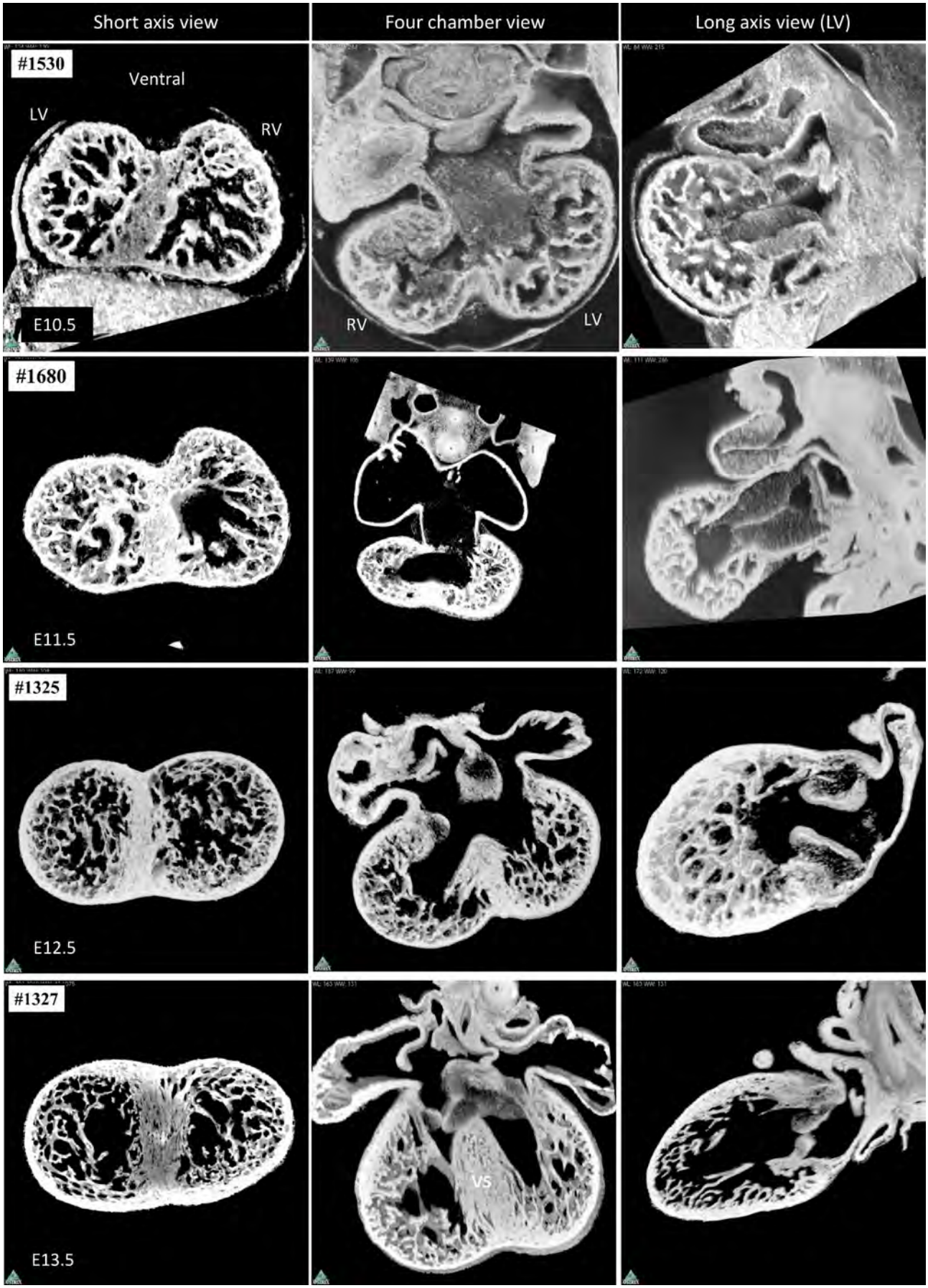

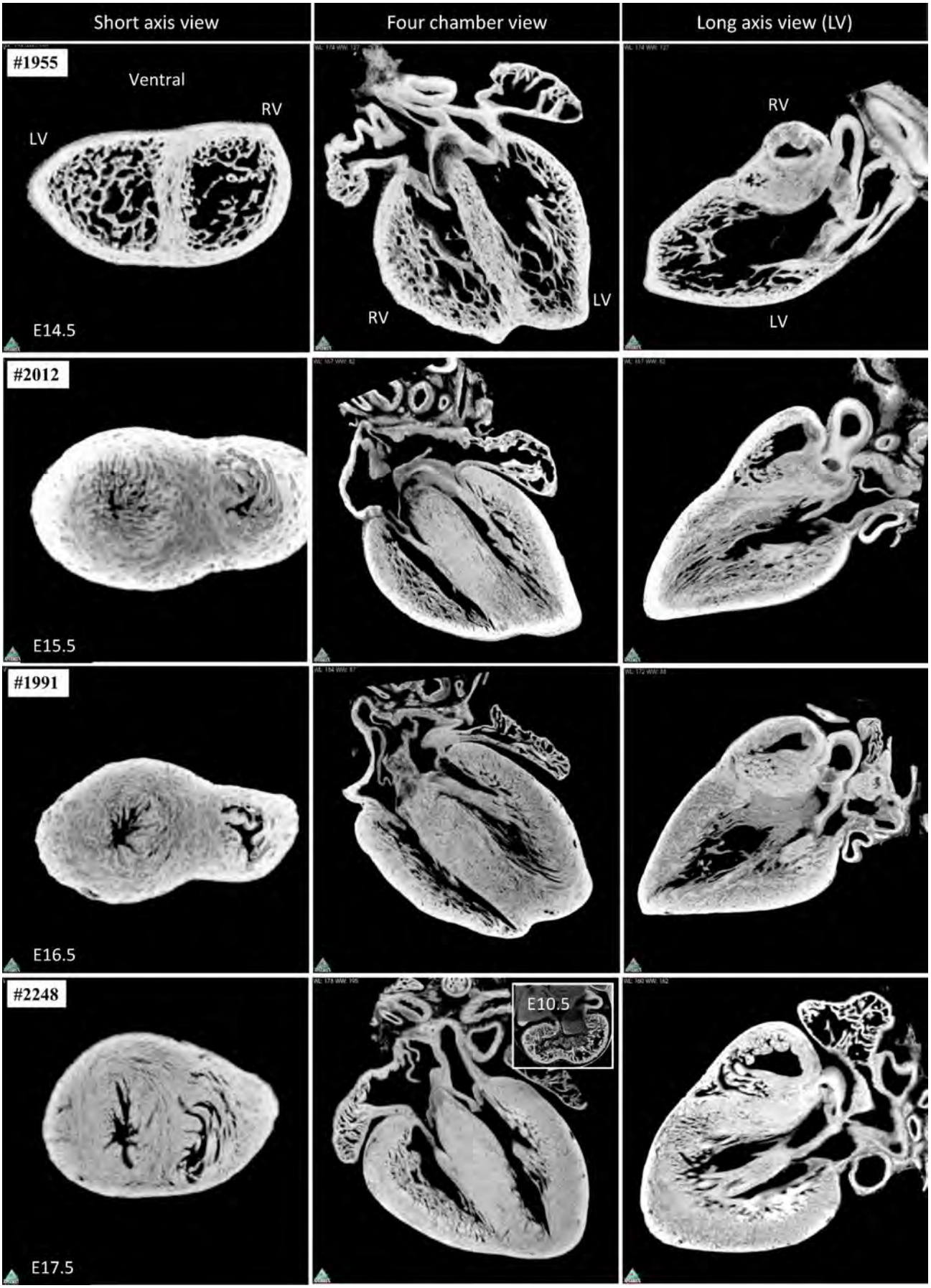

FIGURE 5 Fetal development of the ventricular walls of mouse. The images show the changes occurring from embryonic (E) day 14.5 through day 17.5. As for Figure 4, the columns show the orthogonal views through the ventricle. The panel with the 4-chamber view from the E17.5 period also contains the equivalent view of the heart of the E10.5 period, shown on the same absolute scale. LV, left ventricle; RV, right ventricle.

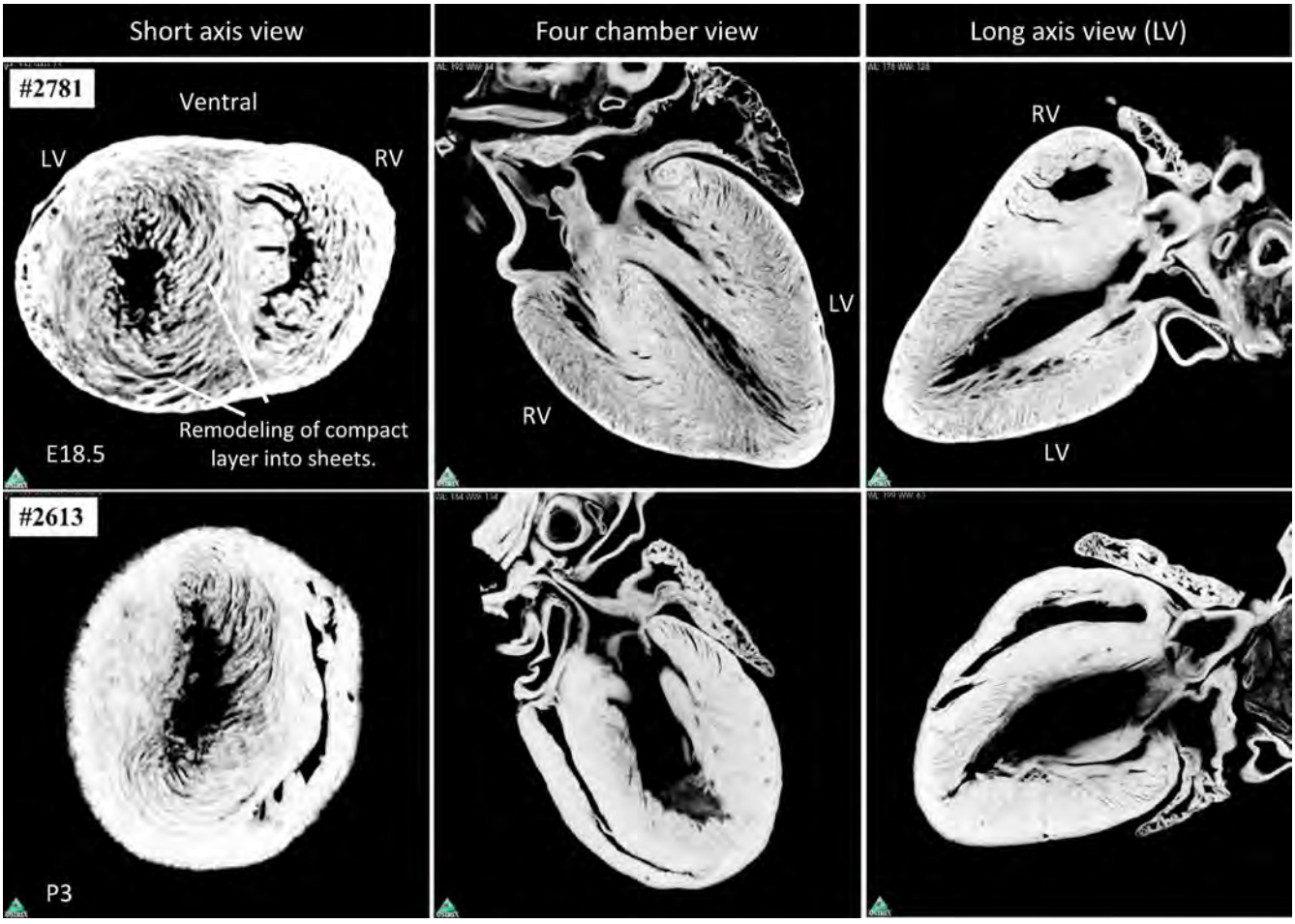

FIGURE 6 Perinatal development of the ventricular walls of mouse. The images, with the columns showing the orthogonal sections through the ventricle as used also for Figures 4 and 5, compare the changes from embryonic (E) day 18.5, shown in the upper row, which is the end of gestation in the mouse, to the third postnatal (P3) day, shown in the bottom row. LV, left ventricle; RV, right ventricle.

which is considered to be the least trabeculated part of the ventricle (Figure 7).

3.3 | Morphological description of human ventricular wall development

Figure 8 shows four periods of human gestation, from Carnegie stage 11 when the ventricular cavity is tiny, over a late embryonic stage at which time the ventricular septation is complete (Carnegie stage 20), to the early fetal period. In the early stages, from Carnegie stages 11 to 14, the ventricular walls are composed primarily of trabecular myocardium, which is visually apparent in Figure 8 and which has been quantified previously as a period of rapid growth (Faber, D'Silva, et al., 2021; Faber, Hagoort, et al., 2021). By Carnegie stage 20, the heart is much bigger, the compact wall is thicker, the central cavity has expanded and the trabecular layer is proportionally reduced, whereas in absolute size the trabecular layer has grown substantially. For the 11th week since conception or the 3rd week of fetal development, the heart shown in Figure 8 shows a pronounced, albeit not complete, morphological resemblance to the adult heart. Thus, the trabecular layer grows for every older stage, but not as much as the compact wall thickens and the central cavity expands.

4 | DISCUSSION

Our data support the notion that different rates of growth of the trabecular and compact layers are the major drivers of the changes that take place in ventricular mural architecture. Compaction may seem to be an important factor if we look solely at the proportional reduction of the trabecular layer thickness. The interpretation of

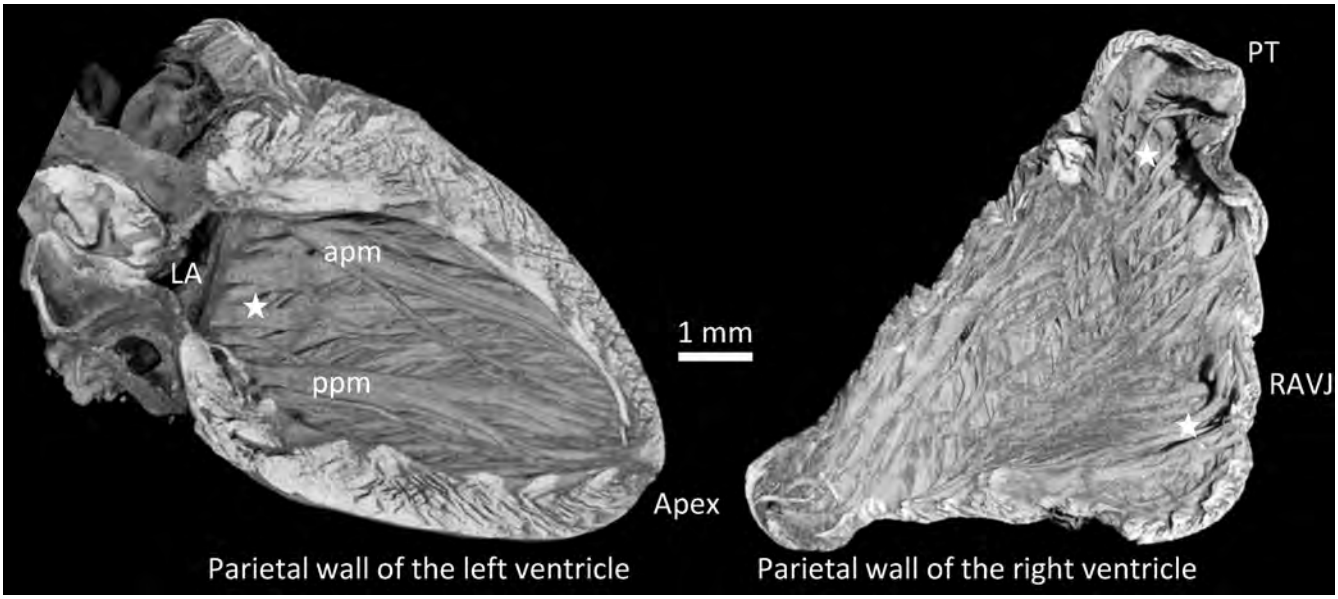

FIGURE 7 Extensive trabeculation in the adult mouse ventricles. The images show the free wall of the adult mouse ventricles, reconstructed from micro-CT datasets. While the ventricular base is considered the least trabeculated part of the ventricle, it nonetheless contains extensive trabeculation (see the area around the star). apm, anterior papillary muscle; LA, left atrium; ppm, posterior papillary muscle; PT, pulmonary trunk; RAVJ, right atrioventricular junction.

compaction as a major driver of morphological change, however, is confounded by several factors that occur simultaneously.

First among these is the absolute scale. The heart grows rapidly, and the number of cardiomyocytes increases from a few tens of thousands to approximately 1 million in the period compaction is said to occur in mouse (de Boer et al., 2012; Faber, Hagoort, et al., 2021). If images of fetal hearts are scaled down, and juxtaposed to microscopic embryonic hearts, for example (Oechslin & Jenni, 2011), this is in effect a reduction of the spatial resolution of the fetal hearts. So, while the fetal trabecular layer may seem to have flattened, in fact, the volume of trabeculations and intertrabecular recesses is greater in the fetal hearts. The impact of scale on spatial resolution, nonetheless, does not explain all the differences. Several factors are again in play. Some flattening of trabeculations likely occurs, most plausibly on the surface of the ventricular septum. A process of flattening can arguably be gleaned from the lineage tracing of Sema3a-expressing myocardium. This myocardium constitutes a trabecular meshwork to the left of the septum at E12.5, but forms only a thin sub-endocardial layer after birth (Tian et al., 2017). This flattening happens at a time when the ventricular cavities expand. The expansion may contribute to thin the trabecular layer while it is growing. This can be compared to making the base of a pizza from a lump of dough. With regard to the recesses, some may collapse and disappear, as suggested by lineage tracing of endocardium that gives rise to coronary endothelium (Tang et al., 2022). At the endpoint, however, the ventricle of the adult has such an extensive and intricate trabecular layer that it is exceedingly difficult to count the number of trabeculations or recesses, either in humans (Gerger et al., 2013; Riekerk et al., 2022) or in mice as we show in this report. While the extent of the trabecular layer is difficult to miss during postmortem macroscopic inspection, the degree of trabeculation is most frequently assessed during life by echocardiography and magnetic resonance imaging. These modalities, at present, do not have sufficient spatial resolution to show all trabeculations and recesses (Jensen & Petersen, 2022; Polacin et al., 2022; Riekerk et al., 2022).

The state of contraction is a second factor that affects the interpretation of the extent of the trabecular layer, also when embryos and fetuses are compared (Ishiwata et al., 2003). The embryonic ventricle will often appear to be in a somewhat diastolic state. Many fetal ventricles, however, will appear in a state of systole. Our own quantifications of the ratio of cavity-to-myocardial volume support this interpretation. If the fetal trabecular layer is relatively compressed, the intertrabecular recesses may appear to have diminished in number, if not disappeared. Previously, mouse hearts were perfusion-fixed under known preload pressure. It was found that both the trabecular and compact layers grew throughout development (Ishiwata et al., 2003). The importance of state of contraction is similarly well recognized when using clinical techniques, such as magnetic resonance imaging. The border between the trabecular and compact layers is relatively easy to identify in diastole, whereas in systole the intertrabecular recesses can become so compressed that part of the trabecular layer can be mistaken for the compact wall (Grothoff et al., 2012). In our assessment, a greater state of contraction likely biases the transmural appearance towards one that suggests extensive compaction.

The third factor worthy of emphasis is the great changes that happen to the structures and spaces that surround the trabecular layer. It is during the period of greatest proportional decline of the trabecular layer (E13.5–17.5 in our mouse data sets), that the compact wall grows most rapidly, and the central cavity expands. From a

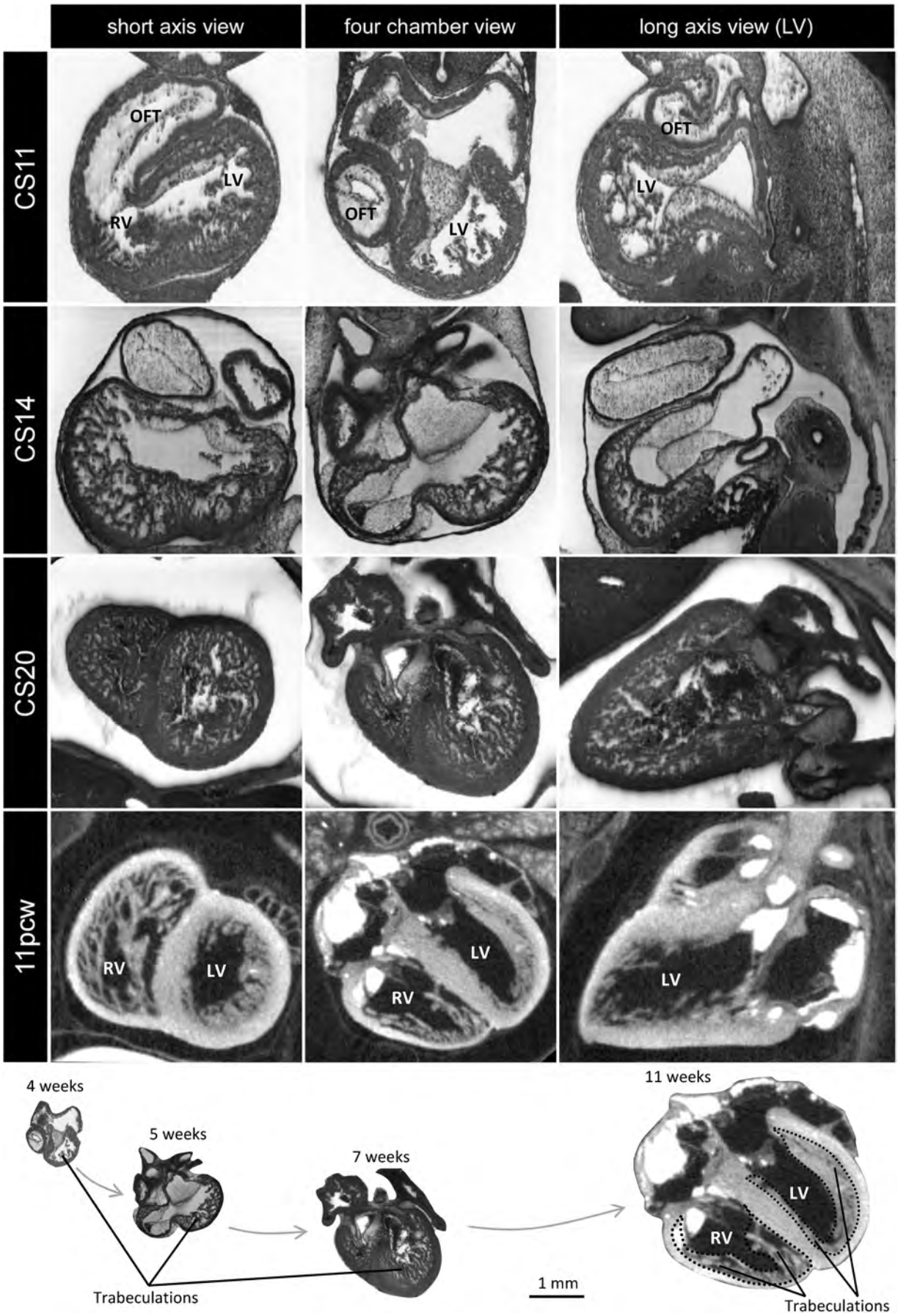

FIGURE 8 Embryonic and early fetal development of the ventricular walls of human. The bottom row shows the 'four chamber' views on the same scale from which it is apparent that the trabecular layer is greater for each stage. LV, left ventricle; OFT, outflow tract; RV, right ventricle.

point of view of cardiac output, rapid growth of the ventricular wall is unsurprising, since the rapidly growing embryo and fetus at that period require a matching cardiac output. Soon after the beating has commenced, the heart rate is almost constant. In mouse, it increases from some 150 beats per minute around E10.5 to approximately 200 beats per minute around E18.5 (Tyser & Srinivas, 2020). In humans, the heart rate becomes almost 200 near the end of the embryonic development. It then stabilizes close to 150 beats per minute in the second trimester (Manner, 2022). In contrast, during the same periods in mouse and human, the myocardial volume increases manyfold. The number of cardiomyocytes, furthermore, increases from a few tens of thousands to about a million (de Boer et al., 2012; Faber, Hagoort, et al., 2021). Consequently, cardiac output in the growing embryo and fetus is sustained for the most part by an increase in the size of the heart, more specifically the stroke volume (Jensen & Smith, 2018). The ventricular cavities must expand accordingly (Faber, Buijtendijk, et al., 2022). The ventricular walls must then grow to maintain systolic pressure, in accordance with the law of Laplace (Buffinton et al., 2013). In this regard, the systolic blood pressure is known to increase with development (Ishiwata et al., 2003; Van Mierop & Bertuch Jr., 1967). In short, if the trabecular layer is assessed in proportion to the ventricular cavity and the compact wall, note must be taken of how much and how fast, there is a shift in these baselines. It is plausible that the expansion of the central cavity goes a long way to explain how the trabeculations come to be laid down on the sides of the base of the ventricular septum.

A fourth factor for emphasis is that trabeculations can themselves coalesce to become fewer, yet of greater size, without impacting on the dimensions of the compact wall (Henderson & Anderson, 2009). Or, at the risk of creating an oxymoron, there can be compaction within the trabecular layer. Papillary muscles are the prime example of this process. From the beginning of development, trabeculations extend between the atrioventricular cushions, from which the leaflets will develop, and the compact wall (de Lange et al., 2004). In the adult hearts of humans and mice, the papillary muscles are between the valve leaflets and their trabecular base (Axel, 2004). While a reduction in the number of trabeculations and intertrabecular recesses is consistent with compaction, the development of the papillary muscle exemplifies that the same morphometric readout is equally consistent with the coalescence of trabeculations within the trabecular layer. Extensive coalescence of trabeculations within the trabecular layer may occur in pig since the proportional volumes of the trabecular layers are similar between pig and human, while the porcine walls have fewer trabeculations (Jensen et al., 2023).

Besides the confounding factors in assessing the extensiveness of the trabecular layer, in microscopy, there is also a risk of mistaking compact wall for trabeculations. This relates to the fact that the cardiomyocytes of the compact wall become aggregated to form a three-dimensional meshwork during the later stages of fetal gestation (around E17.5–18.5 in our data) and such aggregates can resemble trabeculations on histology. Such myocardial organization likely allows for the aggregates to slide with respect to each other, thus allowing for a greater compression of the compact wall (Smerup et al., 2009). The risk of mistaking such components of the three-dimensional intramural mesh for trabeculations is much reduced with an endocardial-specific stain, such as with antibody detection of endomucin (Gifford et al., 2019).

5 | CONCLUSION

Compaction is a developmental process that can substantially alter the morphology of some structures in some species, such as the right ventricular free wall in chicken (Rychterova, 1971). When assessing the morphological change to the trabecular layers of mice and humans, while a process of compaction may seem to provide an intuitive explanation for the thickening of the compact layer, other major processes are at play in parallel. The expansion of the central cavity is prominent among these, together with the intrinsic growth of the compact layer, the change of scale reflecting the tremendous and rapid overall growth of the heart, the coalescence of trabeculations within the trabecular layer itself and the state of contraction of the walls. We posit that the true magnitude of compaction can only be revealed when account has been taken of these shifting baselines. For ventricular walls that contain a high number of trabeculations, such as the ones found in adult mouse and human, our findings indicate that compaction is unlikely to have played a major role in shaping their morphology.

ACKNOWLEDGEMENTS

None.

CONFLICT OF INTEREST STATEMENT

The authors have no conflicts of interest to declare.

DATA AVAILABILITY STATEMENT

The data that support the findings of this study are available from the corresponding author upon reasonable request.

ORCID

Bjarke Jensen https://orcid.org/0000-0002-7750-8035
Simon D. Bamforth https://orcid.org/0000-0002-5666-4485
Robert H. Anderson https://orcid.org/0000-0001-5163-9021

REFERENCES

Anderson, R.H. & Bamforth, S.D. (2022) Morphogenesis of the mammalian aortic arch arteries. *Frontiers in Cell and Development Biology*, 10, 892900.

Anderson, R.H., Jensen, B., Mohun, T.J., Petersen, S.E., Aung, N., Zemrak, F. et al. (2017) Key questions relating to left ventricular noncompaction cardiomyopathy: is the emperor still wearing any clothes? *The Canadian Journal of Cardiology*, 33, 747–757.

Aung, N., Doimo, S., Ricci, F., Sanghvi, M.M., Pedrosa, C., Woodbridge, S.P. et al. (2020) Prognostic significance of left ventricular noncompaction: systematic review and meta-analysis of observational studies. *Circulation Cardiovascular Imaging*, 13, e009712.

Axel, L. (2004) Papillary muscles do not attach directly to the solid heart wall. *Circulation*, 109, 3145–3148.

Blausen, B.E., Johannes, R.S. & Hutchins, G.M. (1990) Computer-based reconstructions of the cardiac ventricles of human embryos. *American Journal of Cardiovascular Pathology*, 3, 37–43.

Buffinton, C.M., Faas, D. & Sedmera, D. (2013) Stress and strain adaptation in load-dependent remodeling of the embryonic left ventricle. *Biomechanics and Modeling in Mechanobiology*, 12, 1037–1051.

Chang, Y.H., Sheftel, B.I. & Jensen, B. (2022) Anatomy of the heart with the highest heart rate. *Journal of Anatomy*, 241, 173–190.

Chin, T.K., Perloff, J.K., Williams, R.G., Jue, K. & Mohrmann, R. (1990) Isolated noncompaction of left ventricular myocardium. A Study of Eight Cases. *Circulation*, 82, 507–513.

de Bakker, B.S., de Jong, K.H., Hagoort, J., de Bree, K., Besselink, C.T., de Kanter, F.E.C. et al. (2016) An interactive three-dimensional digital atlas and quantitative database of human development. *Science*, 354, aag0053.

de Boer, B.A., van den Berg, G., de Boer, P.A., Moorman, A.F. & Ruijter, J.M. (2012) Growth of the developing mouse heart: an interactive qualitative and quantitative 3D atlas. *Developmental Biology*, 368, 203–213.

de Lange, F.J., Moorman, A.F., Anderson, R.H., Männer, J., Soufan, A.T., de Gier-de Vries, C. et al. (2004) Lineage and morphogenetic analysis of the cardiac valves. *Circulation Research*, 95, 645–654.

Degenhardt, K., Wright, A.C., Horng, D., Padmanabhan, A. & Epstein, J.A. (2010) Rapid 3D phenotyping of cardiovascular development in mouse embryos by micro-CT with iodine staining. *Circulation Cardiovascular Imaging*, 3, 314–322.

Faber, J.W., Buijtendijk, M.F.J., Klarenberg, H., Vink, A.S., Coolen, B.F., Moorman, A.F.M. et al. (2022) Fetal tricuspid valve agenesis/atresia: testing predictions of the embryonic etiology. *Pediatric Cardiology*, 43, 796–806.

Faber, J.W., D'Silva, A., Christoffels, V.M. & Jensen, B. (2021) Lack of morphometric evidence for ventricular compaction in humans. *Journal of Cardiology*, 78, 397–405.

Faber, J.W., Hagoort, J., Moorman, A.F.M., Christoffels, V.M. & Jensen, B. (2021) Quantified growth of the human embryonic heart. *Biology Open*, 10, bio057059.

Faber, J.W., Wüst, R.C.I., Dierx, I., Hummelink, J.A., Kuster, D.W.D., Nollet, E. et al. (2022) Equal force generation potential of trabecular and compact wall ventricular cardiomyocytes. *iScience*, 25, 105393.

Finsterer, J., Stollberger, C. & Towbin, J.A. (2017) Left ventricular noncompaction cardiomyopathy: cardiac, neuromuscular, and genetic factors. *Nature Reviews Cardiology*, 14, 224–237.

Gerger, D., Stollberger, C., Grassberger, M., Gerecke, B., Andresen, H., Engberding, R. et al. (2013) Pathomorphologic findings in left ventricular hypertrabeculation/noncompaction of adults in relation to neuromuscular disorders. *International Journal of Cardiology*, 169, 249–253.

Geyer, S.H., Mohun, T.J. & Weninger, W.J. (2009) Visualizing vertebrate embryos with episcopic 3D imaging techniques. *ScientificWorldJournal*, 9, 1423–1437.

Gifford, C.A., Ranade, S.S., Samarakoon, R., Salunga, H.T., de Soysa, T.Y., Huang, Y. et al. (2019) Oligogenic inheritance of a human heart disease involving a genetic modifier. *Science*, 364, 865–870.

Gould, S.J. (1966) Allometry and size in ontogeny and phylogeny. *Biological Reviews of the Cambridge Philosophical Society*, 41, 587–640.

Gregorovicova, M., Bartos, M., Jensen, B., Janacek, J., Minne, B., Moravec, J. et al. (2022) Anguimorpha as a model group for studying the comparative heart morphology among Lepidosauria: evolutionary window on the ventricular septation. *Ecology and Evolution*, 12, e9476.

Grothoff, M., Pachowsky, M., Hoffmann, J., Posch, M., Klaassen, S., Lehmkuhl, L. et al. (2012) Value of cardiovascular MR in diagnosing left ventricular non-compaction cardiomyopathy and in discriminating between other cardiomyopathies. *European Radiology*, 22, 2699–2709.

Gundersen, H.J., Bendtsen, T.F., Korbo, L., Marcussen, N., Møller, A., Nielsen, K. et al. (1988) Some new, simple and efficient stereological methods and their use in pathological research and diagnosis. *APMIS*, 96, 379–394.

Hanemaaijer, J., Gregorovicova, M., Nielsen, J.M., Moorman, A.F.M., Wang, T., Planken, R.N. et al. (2019) Identification of the building blocks of ventricular septation in monitor lizards (Varanidae). *Development*, 146, dev177121.

Henderson, D.J. & Anderson, R.H. (2009) The development and structure of the ventricles in the human heart. *Pediatric Cardiology*, 30, 588–596.

Hussein, A., Karimianpour, A., Collier, P. & Krasuski, R.A. (2015) Isolated noncompaction of the left ventricle in adults. *Journal of the American College of Cardiology*, 66, 578–585.

Ishiwata, T., Nakazawa, M., Pu, W.T., Tevosian, S.G. & Izumo, S. (2003) Developmental changes in ventricular diastolic function correlate with changes in ventricular myoarchitecture in normal mouse embryos. *Circulation Research*, 93, 857–865.

Jensen, B., Agger, P., de Boer, B.A., Oostra, R.J., Pedersen, M., van der Wal, A.C. et al. (2016) The hypertrabeculated (noncompacted) left ventricle is different from the ventricle of embryos and ectothermic vertebrates. *Biochimica et Biophysica Acta*, 1863, 1696–1706.

Jensen, B. & Petersen, S.E. (2022) Making less of a mess of the trabecular mesh. *Radiology: Cardiothoracic Imaging*, 4, e220227.

Jensen, B., Salvatori, D., Schouten, J., Meijborg, V.M.F., Lauridsen, H. & Agger, P. (2024) Trabeculations of the Porcine and Human Cardiac Ventricles Are Different in Number but Similar in Total Volume. *Clinical Anatomy*. https://doi.org/10.1002/ca.24135

Jensen, B. & Smith, T.H. (2018) Examples of weak, if not absent, Form-Function Relations in the Vertebrate Heart. *Journal of Cardiovascular Devlopment and Disease*, 5, 46.

Jensen, B., Wang, T., Christoffels, V.M. & Moorman, A.F. (2013) Evolution and development of the building plan of the vertebrate heart. *Biochimica et Biophysica Acta*, 1833, 783–794.

Luu, J.M., Gebhard, C., Ramasundarahettige, C., Desai, D., Schulze, K., Marcotte, F. et al. (2022) Normal sex and age-specific parameters in a multi-ethnic population: a cardiovascular magnetic resonance study of the Canadian Alliance for healthy hearts and minds cohort. *Journal of Cardiovascular Magnetic Resonance*, 24, 2.

Manner, J. (2022) When does the human embryonic heart start beating? A review of contemporary and historical sources of knowledge about the onset of blood circulation in man. *Journal of Cardiovascular Devlopment and Disease*, 9(6), 187.

Moorman, A.F. & Christoffels, V.M. (2003) Cardiac chamber formation: development, genes, and evolution. *Physiological Reviews*, 83, 1223–1267.

Oechslin, E. & Jenni, R. (2011) Left ventricular non-compaction revisited: a distinct phenotype with genetic heterogeneity? *European Heart Journal*, 32, 1446–1456.

Olejnickova, V., Kocka, M., Kvasilova, A., Kolesova, H., Dziacky, A., Gidor, T. et al. (2021) Gap junctional communication via Connexin43 between Purkinje fibers and working myocytes explains the Epicardial activation pattern in the postnatal mouse left ventricle. *International Journal of Molecular Sciences*, 22(5), 2475.

Petersen, S.E., Jensen, B., Aung, N., Friedrich, M.G., McMahon, C., Mohiddin, S.A. et al. (2023) Excessive Trabeculation of the left ventricle: JACC: cardiovascular imaging expert panel paper. *JACC: Cardiovascular Imaging*, 16, 408–425.

Polacin, M., Karolyi, M., Wilzeck, V., Eberhard, M., Gotschy, A., Alkadhi, H. et al. (2022) Three-dimensional whole-heart cardiac MRI sequence for measuring Trabeculation in left ventricular noncompaction. *Radiology: Cardiothoracic Imaging*, 4, e220109.

Riekerk, H.C.E., Coolen, B.F., Strijkers, G.J. et al. (2022) Higher spatial resolution improves the interpretation of the extent of ventricular trabeculation. *Journal of Anatomy*, 240, 357–375.

Ross, S.B., Jones, K., Blanch, B., Puranik, R., McGeechan, K., Barratt, A. et al. (2020) A systematic review and meta-analysis of the

prevalence of left ventricular non-compaction in adults. *European Heart Journal*, 41, 1428–1436.

Rowlatt, U. (1990) Comparative anatomy of the heart of mammals. *Zoological Journal of the Linnean Society*, 98, 73–110.

Rychterova, V. (1971) Principle of growth in thickness of the heart ventricular wall in the chick embryo. *Folia Morphol (Praha)*, 19, 262–272.

Sankova, B., Benes, J., Jr., Krejci, E., Dupays, L., Theveniau-Ruissy, M., Miquerol, L. et al. (2012) The effect of connexin40 deficiency on ventricular conduction system function during development. *Cardiovascular Research*, 95, 469–479.

Sedmera, D., Grobety, M., Reymond, C., Baehler, P., Kucera, P. & Kappenberger, L. (1999) Pacing-induced ventricular remodeling in the chick embryonic heart. *Pediatric Research*, 45, 845–852.

Sedmera, D., Reckova, M., DeAlmeida, A., Coppen, S.R., Kubalak, S.W., Gourdie, R.G. et al. (2003) Spatiotemporal pattern of commitment to slowed proliferation in the embryonic mouse heart indicates progressive differentiation of the cardiac conduction system. *Anatomical Record Part A, Discoveries in Molecular, Cellular, and Evoloutionary Biology*, 274, 773–777.

Shi, W., Scialdone, A.P., Emerson, J.I., Mei, L., Wasson, L.K., Davies, H.A. et al. (2023) Missense mutation in human CHD4 causes ventricular noncompaction by repressing ADAMTS1. *Circulation Research*, 133, 48–67.

Smerup, M., Nielsen, E., Agger, P., Frandsen, J., Vestergaard-Poulsen, P., Andersen, J. et al. (2009) The three-dimensional arrangement of the myocytes aggregated together within the mammalian ventricular myocardium. *Anatomical Record (Hoboken)*, 292, 1–11.

Tang, J., Zhu, H., Tian, X., Wang, H., Liu, S., Liu, K. et al. (2022) Extension of endocardium-derived vessels generate coronary arteries in neonates. *Circulation Research*, 130, 352–365.

Tian, X., Li, Y., He, L., Zhang, H., Huang, X., Liu, Q. et al. (2017) Identification of a hybrid myocardial zone in the mammalian heart after birth. *Nature Communications*, 8, 87.

Tyser, R.C.V. & Srinivas, S. (2020) The first heartbeat-origin of cardiac contractile activity. *Cold Spring Harbor Perspectives in Biology*, 12(7), a037135.

van der Ven, J.P.G., Sadighy, Z., Valsangiacomo Buechel, E.R., Sarikouch, S., Robbers-Visser, D., Kellenberger, C.J. et al. (2020) Multicentre reference values for cardiac magnetic resonance imaging derived ventricular size and function for children aged 0-18 years. *European Heart Journal Cardiovascular Imaging*, 21, 102–113.

Van Mierop, L.H. & Bertuch, C.J., Jr. (1967) Development of arterial blood pressure in the chick embryo. *Am. The Journal of Physiology*, 212, 43–48.

van Weerd, J.H. & Christoffels, V.M. (2016) The formation and function of the cardiac conduction system. *Development*, 143, 197–210.

Wang, J., Liu, S., Heallen, T. & Martin, J.F. (2018) The hippo pathway in the heart: pivotal roles in development, disease, and regeneration. *Nature Reviews Cardiology*, 15, 672–684.

Wilsbacher, L. & McNally, E.M. (2016) Genetics of cardiac developmental disorders: Cardiomyocyte proliferation and growth and relevance to heart failure. *Annual Review of Pathology*, 11, 395–419.

How to cite this article: Jensen, B., Chang, Y.H., Bamforth, S.D., Mohun, T., Sedmera, D., Bartos, M. et al. (2024) The changing morphology of the ventricular walls of mouse and human with increasing gestation. *Journal of Anatomy*, 00, 1–14. Available from: https://doi.org/10.1111/joa.14017